

MEASURING  $^{12}\text{C}(\alpha, \gamma)^{16}\text{O}$  FROM WHITE DWARF ASTEROSEISMOLOGY

T.S. METCALFE<sup>1</sup>, M. SALARIS<sup>2</sup>, AND D.E. WINGET<sup>3</sup>  
 <travis@ifa.au.dk> <ms@astro.livjm.ac.uk> <dew@astro.as.utexas.edu>  
 Accepted to *The Astrophysical Journal*

## ABSTRACT

During helium burning in the core of a red giant, the relative rates of the  $3\alpha$  and  $^{12}\text{C}(\alpha, \gamma)^{16}\text{O}$  reactions largely determine the final ratio of carbon to oxygen in the resulting white dwarf star. The uncertainty in the  $3\alpha$  reaction at stellar energies due to the extrapolation from high-energy laboratory measurements is relatively small, but this is not the case for the  $^{12}\text{C}(\alpha, \gamma)^{16}\text{O}$  reaction. Recent advances in the analysis of asteroseismological data on pulsating white dwarf stars now make it possible to obtain precise measurements of the central ratio of carbon to oxygen, providing a more direct way to measure the  $^{12}\text{C}(\alpha, \gamma)^{16}\text{O}$  reaction rate at stellar energies. We assess the systematic uncertainties of this approach and quantify small shifts in the measured central oxygen abundance originating from the observations and from model settings that are kept fixed during the optimization. Using new calculations of white dwarf internal chemical profiles, we find a rate for the  $^{12}\text{C}(\alpha, \gamma)^{16}\text{O}$  reaction that is significantly higher than most published values. The accuracy of this method may improve as we modify some of the details of our description of white dwarf interiors that were not accessible through previous model-fitting methods.

*Subject headings:* nuclear reactions, nucleosynthesis, abundances—stars:individual (GD 358)—stars:interiors—stars:oscillations—white dwarfs

## 1. INTRODUCTION

The nuclear reactions responsible for the synthesis of intermediate-mass elements in stars have been known for more than four decades. Although no existing particle accelerator can measure cross-sections for any of these reactions at the low energies relevant to stellar interiors, theoretical methods have been devised to extrapolate from experimental measurements obtained at higher energies. We can only test the validity of these extrapolations indirectly, by predicting the astronomical consequences of a given set of nuclear reaction rates, and then comparing the predictions to observations.

By necessity the astronomical predictions are themselves model-dependent. For example, models of stellar evolution with detailed compilations of nuclear reaction rates have been used to predict the nucleosynthetic yields of various elements, and these were compared to the observed solar abundances to test the accuracy of the rates (Weaver & Woosley 1993). Although this experiment relies on some processes that are not entirely understood (star formation rates, convective mixing and overshoot, supernova explosion mechanisms), it has provided some of the most convincing evidence to date that the extrapolated rates are reasonably accurate.

Such an analysis is simplified by the fact that most of the relevant nuclear reactions have a strong temperature dependence, so large uncertainties in the absolute rates correspond to very small changes to the temperature in models of the stellar interior. The notable exception is the  $^{12}\text{C}(\alpha, \gamma)^{16}\text{O}$  reaction, and so it has been the focus of many experiments in both astronomy and physics.

During helium burning in the core of a red giant, the  $3\alpha$  and  $^{12}\text{C}(\alpha, \gamma)^{16}\text{O}$  reactions compete for the available helium nuclei. The relative rates of the two reactions determines the final yield of oxygen deep in the core. The  $3\alpha$  rate is well established, but the same is not true of the  $^{12}\text{C}(\alpha, \gamma)^{16}\text{O}$  reaction. The extrapola-

tion of its rate to stellar energies is complicated by interference between various contributions to the total cross-section, leading to a relatively large uncertainty (cf. Kunz et al. 2002). This translates into similarly large uncertainties in our understanding of every astrophysical process that depends on this reaction, from supernovae explosions to galactic chemical evolution.

## 2. METHOD

Weaver & Woosley (1993) derived a measurement of the  $^{12}\text{C}(\alpha, \gamma)^{16}\text{O}$  cross-section based on the fact that the total oxygen production in high mass stars has a dramatic effect on the yields of many other elements with masses between oxygen and iron. The end-result of any adopted value for the  $^{12}\text{C}(\alpha, \gamma)^{16}\text{O}$  cross-section is a distinct set of abundances produced and distributed during the explosion of the stellar models as supernovae. The optimal value is the one that can most closely reproduce the relative abundances observed in the Sun.

Another probing of stellar evolution provides an independent method of probing the composition of the material in the stellar interior after helium burning. A star that is not massive enough to establish an internal temperature and density sufficient to fuse two carbon nuclei will eventually shed its envelope as a planetary nebula, leaving the exposed core to begin a long life as a white dwarf star. Depending on the composition of its stratified surface layers, an otherwise normal white dwarf will begin pulsating as it cools through one of several distinct ranges of temperature, or instability strips. During this phase, astronomers have an opportunity to probe the stellar interior while it is still intact, using the techniques of asteroseismology.

In the past decade, the observational requirements of white dwarf asteroseismology have been satisfied by the development of the Whole Earth Telescope (WET; Nather et al. 1990), a group of astronomers distributed around the globe who cooperate to observe these stars continuously for up to two weeks at

<sup>1</sup> Theoretical Astrophysics Center, Institute of Physics and Astronomy, Aarhus University, 8000 Aarhus C, Denmark

<sup>2</sup> Astrophysics Research Institute, Liverpool John Moores University, Twelve Quays House, Egerton Wharf, Birkenhead, CH41 1LD, UK

<sup>3</sup> Department of Astronomy, Mail Code C1400, University of Texas, Austin, TX 78712, USA

a time. This instrument has now provided a wealth of seismological data on the different varieties of pulsating white dwarf stars (cf. Winget et al. 1991, 1994; Kleinman et al. 1998).

In an effort to bring the analysis of WET data to the level of sophistication demanded by the observations, Metcalfe, Nather, & Winget (2000) recently developed a new fitting method using a genetic algorithm to determine the optimal model parameters, including the stellar mass ( $M_*$ ), the effective temperature ( $T_{\text{eff}}$ ), and the mass of the surface helium layer ( $M_{\text{He}}$ ). The underlying ideas for genetic algorithms were inspired by Charles Darwin's notion of biological evolution through natural selection. The basic idea is to solve a problem by *evolving* the best solution from an initial set of random guesses. The computer model provides the framework within which the evolution takes place, and the individual parameters controlling it serve as the genetic building blocks. Observations provide the selection pressure. In practice, this method can be much more efficient than other comparably global techniques, and provides an objective determination of the optimal set of model parameters along with some indication of the uniqueness.

Using this new approach Metcalfe, Winget, & Charbonneau (2001, hereafter MWC) derived an optimal value for the central oxygen mass fraction in the pulsating white dwarf GD 358 using a simple parameterization of the internal oxygen profile. This parameterization fixed the oxygen mass fraction to its central value ( $X_{\text{O}}$ ) out to some fractional mass ( $q$ ) where it then decreased linearly in mass to zero oxygen at  $0.95 m/M_*$ . The statistical uncertainties on these two parameters were determined by calculating a grid of 10,000 models forming all combinations of  $X_{\text{O}}$  and  $q$ , with the other three parameters fixed at their optimal values since none of them showed any correlation with  $X_{\text{O}}$ . The internal  $1\sigma$  uncertainties were then defined by the range of models with root-mean-square (rms) residuals that differed from the optimal solution by less than the statistical uncertainties on the observed periods (quantified by Metcalfe, Nather, & Winget 2000). MWC then derived a preliminary value of the astrophysical S-factor at 300 keV ( $S_{300}^{\text{MWC}} = 290 \pm 15$  keV b) for the  $^{12}\text{C}(\alpha, \gamma)^{16}\text{O}$  reaction by extrapolating the calculations of Salaris et al. (1997) to the mass and oxygen abundance of the optimal model for GD 358 ( $X_{\text{O}} = 0.84 \pm 0.03$ ).

The sensitivity of our pulsation models to the core composition arises through differences in the Brunt-Väisälä (BV) frequency due to changes in the mean molecular weight of the internal mix of ions. For the purposes of illustration, consider the idealized case where the electrons can be treated as a completely degenerate gas and the ions as an ideal gas. As is known, the electron degeneracy pressure is much larger than that due to the ions, and at a given density it is independent of the composition (C and O have the same number of electrons per nucleon). The only non-zero contribution to the BV frequency ( $N^2$ ) must therefore come from the partial pressure of the ions, and for an ideal gas this leads to  $N^2 \propto \rho T / \mu_{\text{ion}}$ , where  $\mu_{\text{ion}}$  is the mean molecular weight of the ions. Consequently, the BV frequency is lower in O-core models ( $\mu_{\text{ion}} = 16$ ) relative to C-core models ( $\mu_{\text{ion}} = 12$ ). Of course, the electrons are not completely degenerate and also contribute a non-negligible amount to the BV frequency, which tends to reduce the magnitude of this effect. For parameters similar to the optimal model for GD 358, O-core models have a BV frequency that is lower by  $\sim 10\%$  in the inner 95% of the stellar mass compared to C-core models. Since this influences such a large fraction of the mass, the net effect on the periods is nearly as significant as the effect of the

envelope He/C interface (cf. Montgomery, Metcalfe & Winget 2001, Fig.4).

### 3. SYSTEMATIC UNCERTAINTIES

In this paper we examine the various contributions to the systematic uncertainty on the measurement of  $X_{\text{O}}$ , including those originating from the observations themselves and from the theoretical models used to interpret them. The latter category includes contributions from the settings of the white dwarf evolution/pulsation models, and from the models used to produce new white dwarf internal chemical profiles (following Salaris et al. 1997) that match the derived value of  $X_{\text{O}}$ .

#### 3.1. Observational Data

GD 358 has been the target of three coordinated observing campaigns by the WET. The first campaign occurred in 1990, and the results (reported in Winget et al. 1994) were the observational basis for the global model-fitting of MWC because more pulsation modes were observed in 1990 than during the other two campaigns. The results of the second campaign in 1994 were reported in Vuille et al. (2000), and the data from the third campaign in 2000 are still undergoing analysis. Although the power spectra resulting from the three campaigns differ substantially—with modes changing their relative amplitudes and sometimes falling below the sensitivity of the observations—the underlying normal mode structure appears to be remarkably stable (see Table 1).

To assess the systematic uncertainty on the optimal model parameters due to the observational data, we repeated the global model-fitting procedure of MWC using the periods and period-spacings from the other two campaigns on GD 358. For the 1994 data we used the  $\ell = 1, m = 0$  modes listed in Table 3 of Vuille et al. (2000) together with the 1990 values for the  $k = 10, 11, 12$  modes, which had no reliable identification in the second campaign. Despite some significant differences in the power spectrum of the third campaign, most of the  $\ell = 1, m = 0$  modes present in 1990 were also detected in 2000, which we combined with the 1990 values for  $k = 11, 12, 15$ . Although the three data sets are not entirely independent, this procedure should provide some information about the systematic uncertainties due to subtle differences in the observational data.

The differences between the optimal set of model parameters from MWC ( $T_{\text{eff}} = 22,600$  K,  $M_* = 0.650 M_{\odot}$ ,  $\log[M_{\text{He}}/M_*] = -2.74$ ,  $X_{\text{O}} = 0.84$ ,  $q = 0.49$ ) and the results of new fits to these two additional data sets are shown in Table 2 [Fits *a* and *b*]. Also listed are differences for a new fit to the 1990 data supplemented by the identifications for  $k = 19, 20, 21$  from Bradley (1993) [Fit *c*], and for a subset of the 1990 data using observations from only one telescope site [McDonald Observatory, Fit *d*]. The latter fit demonstrates that a multi-site campaign is necessary for an accurate determination of the internal composition from ground-based observations. For each fit we also list the rms differences between the observed and calculated periods ( $\sigma_P$ ) and period spacings ( $\sigma_{\Delta P}$ ). For comparison, the optimal fit from MWC had  $\sigma_P = 1.28$  s and  $\sigma_{\Delta P} = 1.42$  s.

#### 3.2. Pulsation Model Settings

There are a number of settings in the evolution/pulsation models used by MWC that were held constant during the optimization procedure. These fixed settings included: [1] the fractional mass of the boundary between the fully self-consistent

TABLE 1  
OBSERVATIONAL DATA SETS FOR GD 358

k	WET 1990 <sup>1,2</sup>	WET 1994 <sup>3</sup>	WET 2000 <sup>a</sup>	McD 1990
8...	423.27	423.26	423.24	422.58
9...	464.23	464.23	464.25	464.25
10...	501.59	501.59 <sup>b</sup>	501.20	502.50
11...	541.75	541.75 <sup>b</sup>	541.75 <sup>b</sup>	538.31
12...	576.76	576.76 <sup>b</sup>	576.76 <sup>b</sup>	571.31
13...	618.28	617.88	618.44	616.11
14...	658.35	657.91	658.62	657.11
15...	700.64	701.06	700.64 <sup>b</sup>	700.62
16...	734.30	733.96	734.19	736.20
17...	770.67	770.58	771.25	770.74
18...	810.7	809.37	811.19	808.63
19...	854.8 <sup>c</sup>	-	-	-
20...	894.2 <sup>c</sup>	-	-	-
21...	943.5 <sup>c</sup>	-	-	-

<sup>a</sup>Results of preliminary data analysis.

<sup>b</sup>Adopted value from WET 1990.

<sup>c</sup>Included for Fit *c* (see Table 2).

REFERENCES—(1) Winget et al. (1994); (2) Bradley (1993); (3) Vuille et al. (2000)

core and the envelope of the models ( $q_{\text{env}}$ ), [2] the fractional mass where the oxygen abundance is fixed to zero ( $q_0$ ), [3] the prescription for convection (fixed to ML3), [4] the diffusion coefficients that describe the He/C interface in the envelope (fixed at  $\alpha_{3,4} = \pm 3$ ), and [5] the energy losses due to neutrinos ( $E_\nu$ ).

We determined the magnitude of systematic uncertainties due to these fixed settings by repeating the 5-parameter global model-fitting procedure of MWC with the settings fixed at alternate values. Anticipating that the shifts to the optimal model parameters would be relatively small, we were able to complete the calculations in fewer iterations than MWC without sacrificing the accuracy of the final solution.

After changing one of the fixed model settings, we fixed  $q$  at its value from MWC ( $0.49 m/M_*$ ) and performed 10 runs of the genetic algorithm. We then temporarily fixed  $T_{\text{eff}}$ ,  $M_*$ , and  $M_{\text{He}}$  to their optimal values from this first iteration and computed a small grid of models with a range of  $X_{\text{O}}$  and  $q$  around their optimal values. If a better fit existed in this grid with a different value of  $q$ , we performed a new set of genetic algorithm runs with  $q$  fixed at this better value and repeated the procedure until no better value of  $q$  was found in the small grid. Finally, we fixed the mass to the optimal value from the final iteration with fixed- $q$  and verified that the optimal fixed-mass solution from 10 more runs of the genetic algorithm was identical to that found in the fixed- $q$  case.

Since the final fixed-mass and fixed- $q$  iterations were completely independent, the end result should be just as global as the solution found by MWC. Even with this computational shortcut, the cumulative additional model-fitting performed for this study represents more than 5 GHz-CPU-years of calculation, which was only practical because of the dedicated parallel computers available to this project (cf. Metcalfe & Nather 2000).

Table 3 lists the changes to the optimal set of parameters for the new 5-parameter fits with seven variations to the fixed model settings, along with the corresponding values of  $\sigma_P$  and  $\sigma_{\Delta P}$ . We discuss the details of these changes below.

### 3.2.1. Core-Envelope Boundary

As noted by Metcalfe, Nather, & Winget (2000) the evolutionary calculations for the core of our models are fully self-consistent, but the envelope is treated separately and adjusted to match the boundary conditions at each time step. As a consequence, only the fraction of the mass inside the core/envelope boundary is directly involved in the evolution, and this may lead to systematic errors. MWC used a grid of starter models with this boundary fixed at  $q_{\text{env}} = 0.95 m/M_*$ . Fit *e* in Table 3 is the result of using a new grid of starter models with this boundary fixed further out, at  $q_{\text{env}} = 0.98 m/M_*$ .

### 3.2.2. Zero Oxygen Point

The parameterization of the internal oxygen profiles used by MWC fixed the fractional mass where the oxygen abundance goes to zero at  $q_0 = 0.95 m/M_*$ . They did this because the models cannot presently include oxygen in the envelopes, leading to the constraint that  $q_0 \leq q_{\text{env}}$ . The new grid of starter models with  $q_{\text{env}} = 0.98 m/M_*$  allowed us to move  $q_0$  out further. Fit *f* in Table 3 shows the shift relative to Fit *e* when  $q_0$  is fixed at  $0.98 m/M_*$ .

### 3.2.3. Mixing-Length Prescription

Our evolution/pulsation code can use either the ML1 prescription for convection from Böhm-Vitense (1958), or the prescription of Böhm & Cassinelli (1971) with the mixing-length/pressure scale height ratio set to either 1 or 2, which correspond to ML2 and ML3 respectively. Beauchamp et al. (1999) found that the best internal consistency between optical and IUE-based effective temperature determinations for DB stars can be achieved using a mixing-length/pressure scale height ratio between the standard ML2 and ML3. The optimal model found by MWC assumed ML3 convection. Fits *g* and *h* in Table 3 show the shifts to the optimal parameter values when ML2 or ML1 are used respectively.

TABLE 2  
SYSTEMATIC DIFFERENCES FROM VARIOUS DATA SETS

Fit	Data Set	$\Delta T_{\text{eff}}$	$\Delta M_*/M_\odot$	$\Delta \log(M_{\text{He}}/M_*)$	$\Delta X_{\text{O}}$	$\Delta q$	$\sigma_P$	$\sigma_{\Delta P}$
<i>a</i> ...	1994 run	-	-	-	+0.02	-	1.31	1.37
<i>b</i> ...	2000 run	-	-	-	-0.05	-0.01	1.23	1.49
<i>c</i> ...	extra-k	-100	-	-	+0.08	-	2.28	2.11
<i>d</i> ...	single-site	-	-	-	+0.14	+0.01	1.86	1.50

TABLE 3  
SYSTEMATIC DIFFERENCES FROM PULSATION MODEL SETTINGS

Fit	Setting	$\Delta T_{\text{eff}}$	$\Delta M_*/M_\odot$	$\Delta \log(M_{\text{He}}/M_*)$	$\Delta X_{\text{O}}$	$\Delta q$	$\sigma_P$	$\sigma_{\Delta P}$
<i>e</i> ...	$q_{\text{env}}$	+1200	-0.030	+0.10	+0.11	-0.01	1.46	1.21
<i>f</i> ...	$q_0$	-	-	-	+0.04	-	1.47	1.18
<i>g</i> ...	ML2	+300	-0.010	+0.05	+0.06	-	1.27	1.48
<i>h</i> ...	ML1	+300	-0.010	+0.05	+0.06	-	1.27	1.46
<i>i</i> ...	$\alpha_{3,4}(\pm 2)$	-100	-	+0.05	-0.02	-	1.46	1.45
<i>j</i> ...	$\alpha_{3,4}(\pm 4)$	+100	-	-	-0.02	-0.01	1.26	1.58
<i>k</i> ...	$E_\nu$	-	-	-	-0.05	-0.01	1.27	1.42

### 3.2.4. Diffusion Coefficients

The description of the He/C transition in our model envelopes does not include the effects of time-dependent diffusion directly, as is done by Dehner & Kawaler (1995) and Córscico et al. (2002). Rather, we use a parameterization of the method of Arcoragi & Fontaine (1980) using the trace element approximation with two adjustable diffusion coefficients: one to describe the shape of the profile in the carbon-rich region of the envelope, and the other to describe the shape in the helium-rich region (cf. Montgomery & Winget 2000; Tassoul, Fontaine, & Winget 1990). The equilibrium values for these coefficients are  $\alpha_{3,4} = {}^{+2}_{-2}/3$ , but the absolute values of each of them may be larger, depending on the relative magnitude of the evolutionary and diffusive timescales for a specific model. For the purposes of asteroseismology, these coefficients can be considered free parameters. By choosing coefficients of opposite sign but the same absolute value, we ensure a smooth composition transition profile. This avoids the unphysical mode-trapping features introduced by the equilibrium diffusion values, but still provides a reasonable approximation to the expected profile shape (cf. Bradley, Winget, & Wood 1993, Fig. 2). The diffusion coefficients used by MWC were  $\alpha_{3,4} = \pm 3$ . Fits *i* and *j* in Table 3 show the effect of using coefficients that produce thicker and thinner He/C transition zones, corresponding to  $\alpha_{3,4} = \pm 2$  and  $\alpha_{3,4} = \pm 4$  respectively.

### 3.2.5. Neutrino Losses

The energy losses from neutrino emission can alter the thermal structure of our models slightly, since they cool the deep interior more efficiently than the outer regions of the core. For the optimal model of GD 358 (which has  $\log T_c = 7.52$ ), the neutrino luminosity still amounts to  $\sim 20\%$  of the total luminosity. The effect on the internal temperature is small, with a maximum difference of  $\Delta T/T = 0.25\%$  in the core. At some level, this might have a detectable signature on the pulsation properties of the models. The optimal solution found by MWC relied on the neutrino rates of Itoh et al. (1996). Fit *k* in Table 3 shows the result of ignoring all sources of energy loss due to neutrinos during the white dwarf cooling phase.

### 3.3. Internal Chemical Profile Model Settings

As noted by MWC, converting a measurement of the central oxygen abundance into a more precise constraint on the  ${}^{12}\text{C}(\alpha, \gamma){}^{16}\text{O}$  reaction rate requires new evolutionary calculations. To produce profiles that match the mass and central oxygen abundance of the optimal fit to GD 358, we have used the same method and code described in Salaris et al. (1997), but updated to use the nuclear reaction rates from the NACRE collaboration (Angulo et al. 1999) rather than from Caughlan et al. (1985).

When a white dwarf is being formed in the core of a red giant during helium burning, the  $3\alpha$  and  ${}^{12}\text{C}(\alpha, \gamma){}^{16}\text{O}$  reactions are competing for the available helium nuclei. The relative success of the two reactions is the primary factor in determining the final oxygen abundance in the center of a white dwarf star formed in this way. A secondary factor is the efficiency and extent of mixing. The profile calculations normally include the effects of semiconvection during the central helium burning phase, but optionally allow complete mixing in the convective overshooting region. This is followed by Rayleigh-Taylor rehomogenization prior to the white dwarf cooling phase, which generally redistributes inward the extra oxygen that accumulates near the outer boundary of the central convective region (see Salaris et al. 1997, and references therein).

In this section we quantify the magnitude of systematic uncertainties on the central oxygen abundance in our models of the internal chemical profiles from changes to these and other aspects of the input physics. Figures 1 and 2 show the internal oxygen profiles for  $0.61 M_\odot$  models resulting from the changes we have considered. We discuss the details of these changes below.

#### 3.3.1. Nuclear Reaction Rates

The top two panels of Figure 1 show the effect of the statistical uncertainties on the NACRE reaction rates for the  ${}^{12}\text{C}(\alpha, \gamma){}^{16}\text{O}$  and  $3\alpha$  reactions. In both cases the solid line is the result of using the suggested values for the reaction rates. In Figure 1a, the dotted and dashed lines indicate the profiles

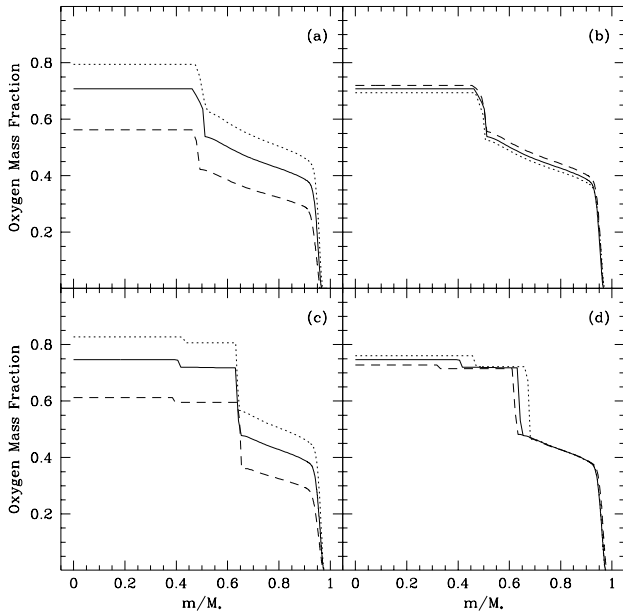


FIG. 1.— Internal oxygen profiles for a  $0.61 M_{\odot}$  white dwarf model using the standard NACRE rates (solid), and (a) using the upper (dotted) and lower (dashed) limits for the  $^{12}\text{C}(\alpha, \gamma)^{16}\text{O}$  rate, (b) using a value for the  $3\alpha$  rate 10 percent higher (dotted) and lower (dashed) than the NACRE value, (c) as in (a) but including convective overshoot with  $\alpha_{\text{ov}}/H_p = 0.20$ , (d) including convective overshoot with  $\alpha_{\text{ov}}/H_p = 0.25$  (dotted) and  $\alpha_{\text{ov}}/H_p = 0.15$  (dashed).

that result when using the upper and lower limits respectively for the  $^{12}\text{C}(\alpha, \gamma)^{16}\text{O}$  reaction, yielding values for the central oxygen abundance between 0.56 and 0.79 ( $\Delta X_{\text{O}} = {}^{+0.08}_{-0.15}$ ).

In Figure 1b, the dotted and dashed lines are the profiles resulting from a value for the  $3\alpha$  rate that is 10 percent higher and lower than the recommended value respectively. This leads to a range of central oxygen abundances from 0.69 to 0.72 ( $\Delta X_{\text{O}} = {}^{+0.01}_{-0.02}$ ).

### 3.3.2. Convective Overshoot

The bottom two panels of Figure 1 show profiles that include the effects of convective overshoot with complete mixing in the overshooting region during central helium burning, rather than standard semiconvective mixing. The profiles in Figure 1c were produced in a similar manner as the corresponding curves in Figure 1a, but include convective overshoot with the overshooting parameter fixed at  $\alpha_{\text{ov}} = 0.20 H_p$ , as suggested by the recent analysis of eclipsing binary data by Ribas, Jordi, & Giménez (2000). With overshoot included, the uncertainty in the  $^{12}\text{C}(\alpha, \gamma)^{16}\text{O}$  reaction leads to values for the central oxygen abundance from 0.61 to 0.82 ( $\Delta X_{\text{O}} = {}^{+0.08}_{-0.13}$ ). The net effect of including convective overshoot on average is to increase the central oxygen abundance at a given  $^{12}\text{C}(\alpha, \gamma)^{16}\text{O}$  rate by  $\Delta X_{\text{O}} = +0.04$ .

In Figure 1d, the dotted and dashed lines are the profiles from higher ( $\alpha_{\text{ov}} = 0.25 H_p$ ) and lower ( $\alpha_{\text{ov}} = 0.15 H_p$ ) assumed values for the overshooting parameter respectively. The central oxygen abundance ranges from 0.73 to 0.76 ( $\Delta X_{\text{O}} = {}^{+0.01}_{-0.02}$ ).

### 3.3.3. Equation of State & Metallicity

In Figure 2 we show the profiles resulting from modifications to two other aspects of the input physics. To produce the dashed line, we computed the progenitor evolution after making an

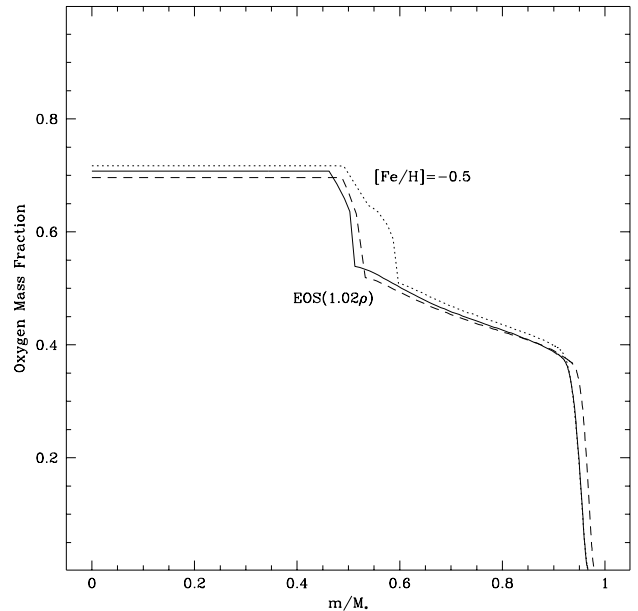


FIG. 2.— The internal oxygen profiles for a  $0.61 M_{\odot}$  white dwarf model using the NACRE rates (solid line), with the density artificially increased by 2 percent (dashed line), and from a progenitor with a metallicity of  $[\text{Fe}/\text{H}] = -0.5$  (dotted line).

*ad hoc* modification to the equation of state (EOS). At fixed values of  $P$  and  $T$  we increased the density by 2 percent. We did not modify the internal energy (the specific heats were unchanged), so the modified EOS has different  $P$ - $T$ - $\rho$  and  $\rho$ - $U$  relationships. Finally, we changed the adiabatic gradient to make it consistent with this pressure and internal energy (cf. Kippenhahn & Weigert 1994). The change in the central oxygen abundance due to this modified EOS is  $\Delta X_{\text{O}} = -0.01$ .

The probable age of GD 358 ( $\sim 0.1$  Gyr) leads us to expect the metallicity of its progenitor to be approximately solar ( $[\text{Fe}/\text{H}] = 0.0$ ). For completeness, we tested the sensitivity of the oxygen profile to changes in the progenitor metallicity. The dotted line in Figure 2 shows the profile from a progenitor with an initial  $[\text{Fe}/\text{H}] = -0.5$ . The primary consequence of this change was to extend the O-rich region, but it also increases the central oxygen abundance by  $\Delta X_{\text{O}} < 0.01$ .

### 3.4. Shape of the C/O Profile

It is clear from the “reverse approach” of MWC that the detailed shape of the internal C/O profile has the potential to reduce the rms residuals of the optimal fit. It is unclear whether the improvement can be considered significant, since the method optimizes the shape of the Brunt-Väisälä frequency directly and is not strictly limited to physically plausible profiles. The parameterization of the internal chemical profile we are using for forward modeling has no physical basis, but was used to facilitate comparison with previous work (cf. Bradley, Winget, & Wood 1993). It is unclear whether our fits would benefit from incorporating a profile with a physical basis because there are still significant differences between the evolutionary profiles computed by various groups. For example, the evolutionary profiles produced by Althaus et al. (2001) contain less structure near  $q \sim 0.5$  than those of Salaris et al. (1997)—apparently due to differences in the treatment of the convective core boundary during helium burning (L. Althaus, private

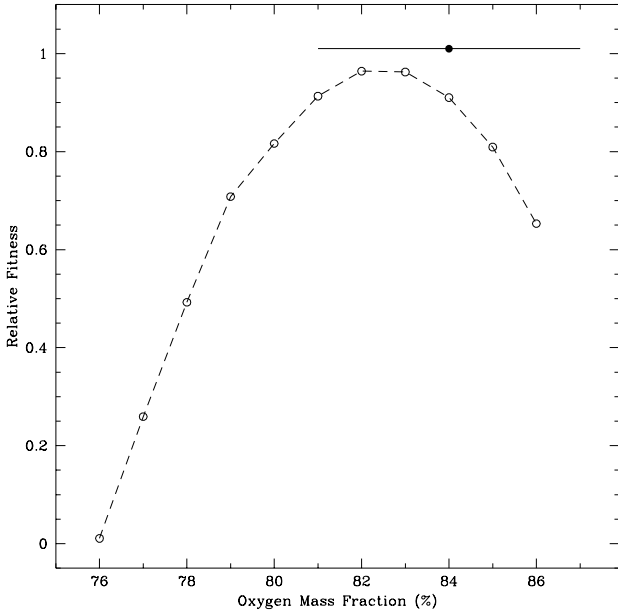


FIG. 3.— The relative quality of the fit to GD 358 using the optimal set of parameters found by MWC, but using an evolutionary internal oxygen profile from the calculations of Salaris et al. (1997) scaled to various values for the central oxygen mass fraction (open points). For comparison we show the optimal value of the central oxygen mass fraction derived from the simple parameterization of the internal oxygen profile used by MWC (solid point; vertical placement is arbitrary).

communication).

To reassure ourselves that the derived values of  $X_O$  are not strongly influenced by the use of non-evolutionary internal chemical profiles, we incorporated the profiles of Salaris et al. (1997) into the optimal model for GD 358 and scaled it to various values of the central oxygen abundance. In Figure 3 we show the relative quality of the fit near the peak fitness for these profiles at  $X_O \sim 0.82$ . For reference, we have shown the optimal value of the central oxygen abundance derived for GD 358 from the simple parameterization of the internal oxygen profile. The *absolute* fitness of the optimal model using an evolutionary profile is much worse, but the peak in the fitness is consistent with the value derived from the simpler profiles ( $\Delta X_O \sim -0.02$ ). While this is reassuring, a more thorough exploration of detailed C/O profiles is certainly warranted in the future.

#### 4. RESULTS

Having demonstrated that the systematic uncertainties from the observations and the model settings are small, we adjusted the value of the  $^{12}\text{C}(\alpha, \gamma)^{16}\text{O}$  rate to match the optimal central oxygen abundance derived for GD 358 by MWC. In Figure 4, we show profiles for  $0.65 M_\odot$  models using the range of rates for the  $^{12}\text{C}(\alpha, \gamma)^{16}\text{O}$  reaction recommended by the NACRE collaboration ( $S_{300}^{\text{NACRE}} = 200 \pm 80$  keV b), and with rates that produce a central oxygen abundance within the  $\pm 1\sigma$  limits for GD 358. The NACRE rates lead to a range for the central oxygen abundance between 0.53 to 0.78, with a value of 0.69 at the recommended rate. To match the central oxygen abundance of GD 358 ( $X_O = 0.84 \pm 0.03$ ) our models require a value for the astrophysical S-factor at 300 keV of  $S_{300} = 370 \pm 40$  keV b, or slightly lower with convective overshoot included:  $S_{300}^{\text{ov}} = 360 \pm 40$  keV b. Note that both the value and the uncertainty of the S-factor are larger than the preliminary estimate

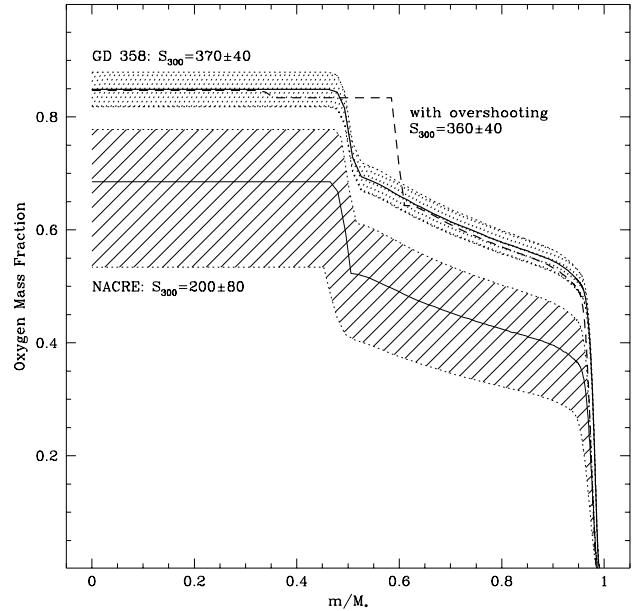


FIG. 4.— The internal oxygen profiles for a  $0.65 M_\odot$  white dwarf model using the NACRE rates (solid line) between the upper and lower limits on the  $^{12}\text{C}(\alpha, \gamma)^{16}\text{O}$  rate (hashed region). Also shown are the profiles resulting from the rates that match the central oxygen mass fraction derived for GD 358 (dark solid line) with the  $\pm 1\sigma$  limits (shaded region), and when overshoot is included (dark dashed line).

of MWC, which was based on an extrapolation from the previously published models of Salaris et al. (1997).

The oxygen profiles in Figures 1 and 4 consistently show the transition from constant oxygen beginning near a fractional mass of  $q \sim 0.5$  when the simulations do not include convective overshoot, regardless of the assumed value for the  $^{12}\text{C}(\alpha, \gamma)^{16}\text{O}$  rate. This is in good agreement with the value of  $q$  found for GD 358 by MWC even though they did not use evolutionary profiles. With convective overshoot included, the transition moves out to  $q \sim 0.6$  and the shape of the profile is otherwise similar. This leads to the exciting possibility that we can use asteroseismology to probe the extent of mixing in the stellar interior. If the progenitor of GD 358 went through normal single-star evolution, then semiconvective mixing appears to be sufficient to explain the optimal internal oxygen profile found by MWC. Complete mixing in the overshooting region is not required.

The ML2 optimal model of GD 358 (Fit g in Table 3) has a mass and temperature closer to the values inferred from spectroscopy by Beauchamp et al. (1999). This was to be expected since they assumed convective parameters that are more similar to ML2 than ML3. An independent observational constraint on the mass and temperature of GD 358 comes from the luminosity implied by its measured parallax (Harrington et al. 1985). The optimal model from our ML2 fit has  $\log(L/L_\odot) = -1.43$ , which is consistent with the value derived from the parallax,  $\log(L/L_\odot) = -1.32^{+0.17}_{-0.27}$  (Bradley & Winget 1994b).

An unexpected result from Table 3 is the relatively small difference in the optimal model parameters from changes to the diffusion coefficients for the He/C transition zone in the envelope. Since the shifts are only 1 or 2 grid points in each parameter, it may be possible to optimize the values of the diffusion coefficients using a relatively small grid search *after* finding the global solution with the genetic algorithm. If the fit can be im-

proved significantly with a different combination of  $\alpha_{3,4}$ , we can fix them to their optimal values in future runs of the genetic algorithm. Eventually, we might begin to achieve rms residuals that approach the level of the observational uncertainties ( $\sigma_{\text{obs}} \sim 0.1$  s).

## 5. DISCUSSION

The rate implied for the  $^{12}\text{C}(\alpha, \gamma)^{16}\text{O}$  reaction from GD 358 is high relative to most published values (cf. Kunz et al. 2002, Table 1). The total cross-section has electric dipole (E1) and quadrupole (E2) components, and a variety of experimental and theoretical methods exist to derive one or both of these contributions. The highest recently published value for the E1 component is  $S_{300}^{E1} = 101 \pm 17$  keV b (Brune et al. 2001), while recent work by Angulo & Descouvemont (2001) on the E2 component suggests a possible value in the range  $S_{300}^{E2} = 190\text{--}220$  keV b. Even if these values ultimately prove to be correct, the total rate would be in the range  $S_{300} = 290\text{--}320$  keV b, and would still be only marginally consistent with the value inferred from GD 358.

Recent work on type Ia supernovae (SNe Ia) also favors a high value for the  $^{12}\text{C}(\alpha, \gamma)^{16}\text{O}$  rate to produce model light curves with a sufficiently slow rise to maximum light (Höflich, Wheeler, & Thielemann 1998). This might even have implications for the determination of cosmological parameters from high redshift SNe Ia (Domínguez, Höflich, & Straniero 2001). Fortunately, there are other observational consequences of the higher rate in the infrared spectra of SNe Ia models, so independent tests should soon be possible (cf. Marion, Höflich, & Wheeler 2001).

If we assume that our method is sound but the value for the  $^{12}\text{C}(\alpha, \gamma)^{16}\text{O}$  rate we have obtained is not accurate, the simplest explanation is that we have failed to optimize something in our model, which leads us to a biased estimate of the central oxygen abundance. In §3, we have demonstrated that many of the fixed model settings do not appear to make much difference to the final set of optimal parameters. This suggests that we may want to revisit some of the more fundamental details of our models to identify the root cause of the discrepancy between our value for the S-factor and the value extrapolated from high-energy laboratory measurements. Below we discuss future areas of investigation and possible improvements to our models that may help us to identify any problems.

The results in Table 3 make it clear that the single most significant improvement we can make to our models is the inclusion of the entire mass, from core to surface, in the evolution calculations. Increasing the core mass from 95 to 98 percent of the total stellar mass changed the optimal value for the central oxygen abundance by 11 percent and simultaneously resulted in an optimal temperature and stellar mass closer to the values for GD 358 inferred from spectroscopy (Beauchamp et al. 1999). However, the shift in the oxygen abundance from this setting by itself leads to a *higher* inferred nuclear reaction rate, not lower.

It is possible that our method is sound, but we are using a model that is incomplete. For example, if the interior of GD 358 contains a significant mass of  $^{22}\text{Ne}$ , our fit could be biased toward a higher central oxygen abundance because it is attempting to create a higher central density using the wrong ingredients. In fact, we calculated the  $^{22}\text{Ne}$  abundance along with the other internal chemical profiles, and found it to be present in the simulations with a mass fraction of  $\sim 3\text{--}5$  percent, depending on the adopted mixing scheme. According to Bild-

sten & Hall (2001), the timescale for gravitational settling of the  $^{22}\text{Ne}$  is much longer than the evolutionary timescale for a DBV white dwarf. If possible, we should include  $^{22}\text{Ne}$  as an adjustable parameter in future fits to pulsation data. Independent observational tests of the core composition may also be possible through measurements of the rate of period change for white dwarf stars with well-isolated pulsation modes (cf. Kepler et al. 2000; Sullivan 2000).

Although we have confirmed that the derived oxygen abundance does not depend strongly on the sharpness of the He/C transition in the envelope, we have not considered a fundamentally different form for the transition zone. One possibility might be the form suggested by Dehner & Kawaler (1995), who included the effects of time-dependent diffusion in their white dwarf models to try to establish a plausible evolutionary connection between the PG 1159 stars and the DBVs. This led to two composition transitions in the envelope: one from pure He to a He/C mixture at a fractional mass near  $10^{-6}$ , and a second between the He/C mixture and the C/O core occurring near  $10^{-2.75} m/M_*$ . Metcalfe, Nather, & Winget (2000) found two families of solutions corresponding approximately to these two layer masses in their initial analysis of GD 358. This possibility merits further investigation, but may not be sufficient in light of the recent detection of C in the atmosphere of GD 358 (Provencal et al. 2000), which cannot be explained by traditional models of carbon dredge-up.

Finally, we could be assuming the wrong evolutionary origin for GD 358. Nather, Robinson, & Stover (1981) suggested that some DB stars may be the end-product of a merged interacting binary white dwarf like the AM CVn systems. The internal oxygen abundances and profiles of such merged objects are unlikely to be the same as their non-binary cousins, and we should be able to distinguish them from one another through asteroseismology. This idea was investigated observationally for AM CVn by Provencal et al. (1995), and some theoretical consequences for DBV stars like GD 358 were quantified by Nitta & Winget (1998). But the latter authors conclude that if GD 358 has a binary origin, it must have gone through an extremely long accretion phase—approaching the theoretical limit.

The biggest problem at the moment is that we have only applied this global model-fitting technique to one pulsating white dwarf, and the other DBV stars have not been observed intensely enough and/or do not exhibit a sufficient number of pulsation modes to allow a reliable analysis. Handler, Wood, & Nitta (2001) and the WET collaboration are currently attempting to remedy this situation. Fortunately, each additional object will provide an independent potential measurement of the  $^{12}\text{C}(\alpha, \gamma)^{16}\text{O}$  rate at stellar energies, and white dwarfs with various masses should have slightly different internal oxygen abundances—but all of them should be consistent with the same underlying nuclear physics.

With the addition of an extra parameter for the H layer mass, it should be possible to extend our method to the (more numerous) DAV white dwarfs, but most of them also suffer from the problem of having too few observed pulsation modes. Kleinman et al. (1998) attempted to overcome this problem by assuming that the underlying mode structure in an individual DAV was stable, and combining all of the frequencies visible in different observing runs into a single list of modes. Clemens (1994) introduced the concept of ensemble asteroseismology by assuming that the DAVs were an approximately uniform class of objects that could be understood collectively, and scaled the

frequencies observed in many different DAVs into a common asteroseismic proto-type. One or both of these techniques may prove to be useful in our future modeling efforts.

We owe special thanks to Mike Montgomery and the anonymous referee for helping us to understand the physical origin of our model sensitivity to the core composition. We thank Ed Nather, Steve Kawaler, and Joergen Christensen-Dalsgaard for helpful discussions. This work was supported in part by the Danish National Research Foundation through its establishment of the Theoretical Astrophysics Center. Computational resources were provided by the University of Texas at Austin, Aarhus University, and by White Dwarf Research Corporation through grants from the Fund for Astrophysical Research and the American Astronomical Society. Financial support was also provided through grant NAG5-9321 from NASA's Applied Information Systems Research Program.

#### APPENDIX

The evolution code we used for the calculations presented here was derived from WDEC, which was most recently described in detail by Wood (1990). Descriptions of more recent updates to the constitutive physics can be found in Bradley (1993) and Montgomery (1998), but for reference we provide an overview of the details that are relevant to our DBV models. The equation of state (EOS) for the cores of our models come from Lamb (1974), and from Fontaine, Graboske & Van Horn (1977) for the envelopes. The C/O mixture in the inter-

rior and the He/C mixture in the envelope are interpolated between pure compositions using the additive volume technique (Fontaine, Graboske & Van Horn 1977). We use an adaptation of the method of Arcoragi & Fontaine (1980) to describe the composition transition zones in the envelope, as described in §3.2.4. We use the updated OPAL opacity tables from Iglesias & Rogers (1993), neutrino rates from Itoh et al. (1996), and the mixing-length prescription of Böhm & Cassinelli (1971). We use the Modified Ledoux treatment of the Brunt-Väisälä frequency described by Tassoul, Fontaine, & Winget (1990), which includes the term that correctly accounts for composition gradients.

We determined the pulsation frequencies of our evolved models using the adiabatic non-radial oscillation code described by Kawaler (1986), which solves the pulsation equations using the Runge-Kutta-Fehlberg method. The periods resulting from the adiabatic approximation typically differ from the non-adiabatic results by only a few thousandths of a second, which is well below the present level of observational noise.

The validity of our DB white dwarf evolution/pulsation models have been investigated by Benvenuto & Althaus (1997), who used their independent state-of-the-art code to verify conclusions made by Bradley & Winget (1994a), which were based on the same code we have used in our study. Benvenuto & Althaus include a more recent convective theory in their models that naturally leads to an efficiency between ML2 and ML3. This difference does not matter in the context of our paper, since we have demonstrated in §3.2.3 the weak dependence of our final result on the convective prescription.

#### REFERENCES

- Althaus, L. G., Serenelli, A. M., Córscico, A. H., Benvenuto, O. G. 2001, MNRAS, accepted  
 Angulo, C. et al. 1999, Nuclear Physics A, 656, 3 [NACRE]  
 Angulo, C. & Descouvemont, P. 2001, Nuclear Physics A, 688, 546  
 Arcoragi, J. & Fontaine, G. 1980, ApJ, 242, 1208  
 Beauchamp, A., Wesemael, F., Bergeron, P., Fontaine, G., Saffer, R. A., Liebert, J. & Brassard, P. 1999, ApJ, 516, 887  
 Benvenuto, O. G. & Althaus, L. G. 1997, MNRAS, 288, 1004  
 Bildsten, L. & Hall, D. M. 2001, ApJ, 549, L219  
 Böhm, K. H. & Cassinelli, J. 1971, A&A, 12, 21  
 Böhm-Vitense, E. 1958, Zeitschrift Astrophysics, 46, 108  
 Bradley, P. A. 1993, Ph.D. thesis, University of Texas-Austin, see PASP, 106, 104  
 Bradley, P. A. & Winget, D. E. 1994a, ApJ, 421, 236  
 Bradley, P. A. & Winget, D. E. 1994b, ApJ, 430, 850  
 Bradley, P. A., Winget, D. E., & Wood, M. A. 1993, ApJ, 406, 661  
 Brune, C. R. et al. 2001, Nuclear Physics A, 688, 263  
 Caughlan, G. R., Fowler, W. A., Harris, M. J., & Zimmerman, B. A. 1985, Atomic Data and Nuclear Data Tables, 32, 197  
 Clemens, J. C. 1994, Ph.D. thesis, University of Texas-Austin, see PASP, 106, 1322  
 Córscico, A. H., Benvenuto, O. G., Althaus, L. G. & Serenelli, A. M. 2002, MNRAS, accepted  
 Dehner, B. T. & Kawaler, S. D. 1995, ApJ, 445, L141  
 Domínguez, I., Höflich, P., & Straniero, O. 2001, ApJ, 557, 279  
 Fontaine, G., Graboske, H. C., Jr., & Van Horn, H. M. 1977, ApJS, 35, 293  
 Handler, G., Wood, M. A., & Nitta, A. 2001, in proceedings of IAU Coll. 185, Radial and Non-Radial Pulsations as Probes of Stellar Physics, C. Aerts, T. Bedding, and J. Christensen-Dalsgaard, eds., in press  
 Harrington, R. S. et al. 1985, AJ, 90, 123  
 Höflich, P., Wheeler, J. C., & Thielemann, F. K. 1998, ApJ, 495, 617  
 Iglesias, C. A., & Rogers, F. J. 1993, ApJ, 412, 752  
 Itoh, N., Hayashi, H., Nishikawa, A., & Kohyama, Y. 1996, ApJS, 102, 411  
 Kawaler, S. 1986, Ph.D. thesis, University of Texas-Austin  
 Kepler, S. O., Mukadam, A., Winget, D. E., Nather, R. E., Metcalfe, T. S., Reed, M. D., Kawaler, S. D., & Bradley, P. A. 2000, ApJ, 534, L185  
 Kippenhahn, R. & Weigert, A. 1994, Stellar Structure and Evolution, (New York: Springer-Verlag)  
 Kleinman, S. J., et al. 1998, ApJ, 495, 424  
 Kunz, R., Fey, M., Jaeger, M., Mayer, A., Hammer, J. W., Staudt, G., Harissopulos, S., & Paradellis, T. 2002, ApJ, 567, 643.  
 Lamb, D. Q. 1974, Ph.D. thesis, University of Rochester  
 Marion, G. H., Höflich, P., & Wheeler, J. C. 2001, Revista Mexicana de Astronomia y Astrofisica Conference Series, 10, 190  
 Metcalfe, T. S., & Nather, R. E. 2000, Baltic Astronomy, 9, 479  
 Metcalfe, T. S., Nather, R. E. & Winget, D. E. 2000, ApJ, 545, 974  
 Metcalfe, T. S., Winget, D. E., & Charbonneau, P. 2001, ApJ, 557, 1021 [MWC]  
 Montgomery, M. H. 1998, Ph.D. thesis, University of Texas-Austin  
 Montgomery, M. H., Metcalfe, T. S. & Winget, D. E. 2001, ApJ, 548, L53  
 Montgomery, M. H. & Winget, D. E. 2000, Baltic Astronomy, 9, 23  
 Nather, R. E., Robinson, E. L., & Stover, R. J. 1981, ApJ, 244, 269  
 Nather, R. E., Winget, D. E., Clemens, J. C., Hansen, C. J. & Hine, B. P. 1990, ApJ, 361, 309  
 Nitta, A. & Winget, D. E. 1998, Baltic Astronomy, 7, 141  
 Provencal, J. L. et al. 1995, ApJ, 445, 927  
 Provencal, J. L., Shipman, H. L., Thejll, P., & Vennes, S. 2000, ApJ, 542, 1041  
 Ribas, I., Jordi, C., & Giménez, Álvaro 2000, MNRAS, 318, L55  
 Salaris, M., Domínguez, I., Garcia-Berro, E., Hernanz, M., Isern, J. & Mochkovitch, R. 1997, ApJ, 486, 413  
 Sullivan, D. J. 2000, in Proceedings of IAU Colloq. 176, ASP Conf., 203, 523  
 Tassoul, M., Fontaine, G., & Winget, D. E. 1990, ApJS, 72, 335  
 Vuille, F. et al. 2000, MNRAS, 314, 689  
 Weaver, T. A. & Woosley, S. E. 1993, Phys. Rep., 227, 65  
 Winget, D. E., et al. 1991, ApJ, 378, 326  
 Winget, D. E., et al. 1994, ApJ, 430, 839  
 Wood, M. 1990, Ph.D. thesis, University of Texas-Austin